Resonance Phenomenon and Its Effects of Laser Texture Disk

Sung-Hoon Choa*, Geng Wang

Samsung Information System America, USA

To achieve lower flying height for high areal recording density, the laser zone texturing of the disk needs to be designed to reduce glide height. One problem of the laser bump design is that the regular laser bump pattern often produces glide resonance phenomenon, which leads to failure of the glide height test. However, it was found in this study that glide resonance is an intrinsic problem of the glide head used and resonance phenomenon depends on the type of the head slider, that is, the natural frequency of the slider body. Therefore, higher glide height or glide failure caused by glide resonance does not lead to head/media interface problem in the real drive operating conditions in which the data head is used. Pseudo-random bump pattern greatly reduces the glide resonance. Smaller bump pitch will also help to reduce the glide resonance. However, as bump spacing becomes smaller, glide height will be increased due to increased air pressure developed around the bumps. Lowering bump height is the most effect way to reduce glide avalanche.

Key Words : Glide Test, Resonance Phenomenon, Laser Texture Disk, Hard Disk Drive

1. Introduction

The demand for high areal recording density in magnetic hard disk drive (HDD) continuously requires a decrease in the head/disk spacing, i. e., a lower flying height. It is therefore important to have the disk surface topography to be as smooth as possible so that the head can fly safely at such low flying height. On the other hand, the disk surface is also textured to a very tight range in order to prevent stiction during head parking. As a consequence, the laser zone texture (LZT), which has laser induced bump on the disk land- ing zone, has been widely employed as one of the texturing technology in the disk industry (Kuo et al., 1996).

To ensure non-interference between the head and disk even under extreme drive operating conditions, it is necessary to conduct the glide test

* Corresponding Author,
   E-mail : shchoa@sisa.samsung.com
   TEL : +82-331-200-4749 ; **FAX** : +82-331-200-3144
   Samsung Information System America, San Jose, CA95134, USA. (Manuscript **Received** December 10, 1999; **Revised** May, 9, 2000)

to screen the disks for the presence of defects that are taller than a specific flying height (Clark, 1991). During the glide tests, the glide head flies over a disk medium at a predetermined clearance known as the glide height. While the purpose of the glide test is to screen out the disks with taller defects, the topographical features on the disk surface may also interfere with the heads to cause failures. This intrinsic glide capability of a disk is typically assessed by a different test, called glide avalanche test, in which the flying height of a test head is reduced continuously until the head touches down on the disk surface. Therefore glide avalanche determines the minimum safe flying height (Marchon et al., 1996). As a result, the laser zone texture of the disk has to be properly designed to guarantee the minimum flying height between the head and the disk, i. e. to meet a specific glide avalanche requirement. The glide test is typically done by spinning a disk at full speed first, and then gradually reducing the disk rotating speed until head-disk contacts are detect- ed by PZT sensor in the glide head. If the contact occurs between the glide head and a disk defect or asperity, the contact force will excite the slider

and PZT sensor to vibrate. If the voltage from PZT vibration exceeds a predetermined threshold level, the disk is rejected.

During the glide or glide avalanche testing of a laser zone textured (LZT) disk, one often observes many amplified irregular signals which can cause a false reading or failure in glide avalanche measurement. It is known that these irregular peak signals are primarily resulted from excitation of the slide body and the PZT sensor by the periodic laser bump array. Chen et al. (1997) observed that the resonance frequency is a multiple of the bump excitation frequency and a natural frequency of the slider torsional mode. Yao et al. (1998) also investigated the bump excitation through frequency spectrogram analysis. They observed that when the fundamental frequency of the bump array in the regular pattern laser texture intercepts the natural frequencies of the slider/sensor body, the sensor output is amplified, causing false reading in glide testing. Some attempts were suggested to avoid this phenomenon such as use of pseudo-random bump or spiral pattern bump (Yao et al., 1998; Knigge and Talke, 1999). However there is little study about whether glide failure caused by glide resonance phenomenon represents failure of the minimum flying height of the head, consequently leading to the head/media interface problem in the real drive such as when the data head is used. In this study, we investigated the characteristics of resonance phenomenon of the laser bump array by using both glide and data heads, and focused on whether glide resonance can lead to head/media interface problem during take-off or landing operation of the data head. In addition, the design

methods of the laser bump array to achieve lower glide height are discussed.

2. Experimental

Since the bump excitation frequencies vary with the spindle speed during take-off and landing of the slider, an understanding of how frequency spectrum progresses in the time domain is important. A spectrogram is a graph that displays the amplitude of the frequency spectrum versus time. Therefore it is also known as a joint time-frequency analysis. In this study, glide resonance phenomenon was investigated through spectrogram analysis of PZT sensor output using TTi T9000 Glide Tester. The AE signals generated from the PZT glide head were fed to a pre-amp and also connected to a vector signal analyzer that displays the spectrogram. For glide head, Glide-Write 50% PZT slider was used. The schematic configuration of the PZT glide head is shown in Fig. 1. For data head, 50 % (nano) negative pressure slider was used, which has the nominal flying height of 40 nm (1.6 μin) at 5400 rpm. The natural frequencies of the PZT glide
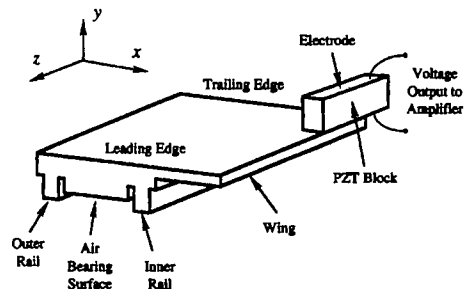

Fig. 1 Geometry of a PZT glide head

Table 1 Design parameters of tested disks

Disk Type	Texture Type	Circumferential Spacing (μm)	Radial Spacing (μm)	Bump Height (Å)
A	Regular	50	25	180
B	Regular	40	25	210
C	Pseudo-random	30*	20	180
D	Regular	30	20	180

*nominal spacing for pseudo-random texture

slider are 360, 420, 680, 800 kHz while the natural frequencies of the data head slider are 720, 890, 1390 kHz. Those data were provided from manufacturers. The head-disk contacts during take-off of the data head were also investigated by monitoring acoustic emission (AE) signal using commercially available contact start/stop (CSS) tester. All the tests including acoustic emission and glide testing were conducted on the laser texture zone of the disk. The disks, obtained from different manufacturers, were made of Al/NiP substrate of 95 mm diameter. They were coated with carbon overcoat, and also lubricated with Z-dol with a nominal thickness of 15 Å. The laser bump shape for all disks was a crater type (or V shape type). The design parameters of the tested disks are listed in Table 1. Bump height and pitch of each disk were measured using atomic force microscopy (AFM).

3. Spectrogram Analysis

Figure 2 shows the spectrogram of type A disk tested with the PZT glide head. The vertical axis represents the frequency, ranging from 0 kHz to 1000 kHz. The horizontal axis represents the flying height, or disk rotational speed ranging from 1200 to 9600 rpm. The amplitude of the frequency spectrum is indicated by the gray-scale of the spectrum. The natural frequencies of the PZT slider are shown in the vertical axis, such as 360, 420, 680, 800 kHz. Line A represents the input excitation frequency from the regular pattern laser bumps, and its harmonics, which are proportional to the spindle rotational frequency.
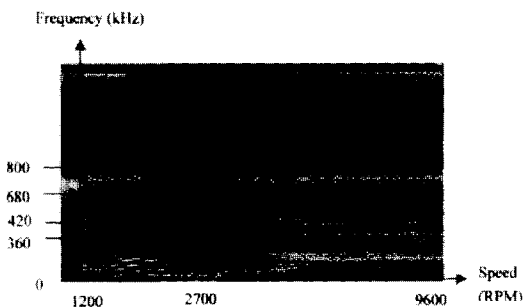

Frequency (kHz)

Fig. 2   Spectrogram of type A disk tested with TTi Glide Tester

When the input excitations intercept the system natural frequencies, they generate a strong response as shown by the circles in Fig. 2.

The excitation frequency f can be calculated by the circumferential bump-spacing (x), the disk linear speed (V), and the testing radius (r) as follows:

$$f = \left(\frac{V}{x}\right) N = \left(\frac{RPM}{60}\right) \times \left(\frac{2\pi r N}{x}\right)$$

here, $N = 1, 2, 3 \cdots$

The factor N includes all the higher order harmonics. This equation represents a set of lines, i. e. Lines A, that pass through the origin in the spectrogram. The excitation frequencies calculated from the equation are found to match the excitation frequencies in the spectrogram. For example, a strong response shown by the circle in Fig. 2 is the third harmonic of the fundamental frequency. That is, for bump spacing of 50 μm, 2700 rpm, testing radius of 20.5 mm, a strong response was detected when N is 3.

4. Glide Resonance Effects

Figure 3 shows the glide avalanche curve (top) and spectrogram (bottom) tested with the glide PZT head for type A disk and type B disk. Type A disk, which has lower bump height than type B disk, showed higher glide avalanche than did type B disk. This is a conflicting result with our expectation since it is generally known that lower bump height would produce lower glide avalanche. As discribed previously, this result is attributed to the glide resonance phenomenon shown in the spectrogram of Fig. 3, where type A disk, which has higher glide resonance, produces higher glide avalanche than the type B disk. However, performance reversal was observed while the glide test was conducted with the data head; type B disk showed higher avalanche than the type A disk as shown in Fig. 4. Here, we could not obtain the spectrogram when the data head was used. In this case the signal was weak and not well defined, therefore it was more difficult to detect the bump frequency accurately. It is thought that the PZT glide head is much more
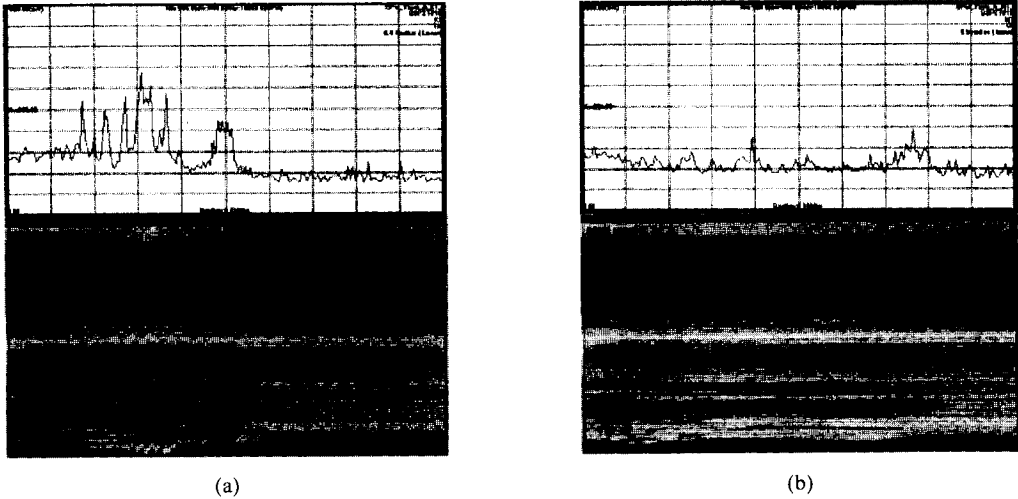
(a)   (b)

Fig. 3 Glide avalanche curve (top) and spectrogram (bottom) for (a) type A disk and (b) type B disk tested with glide head
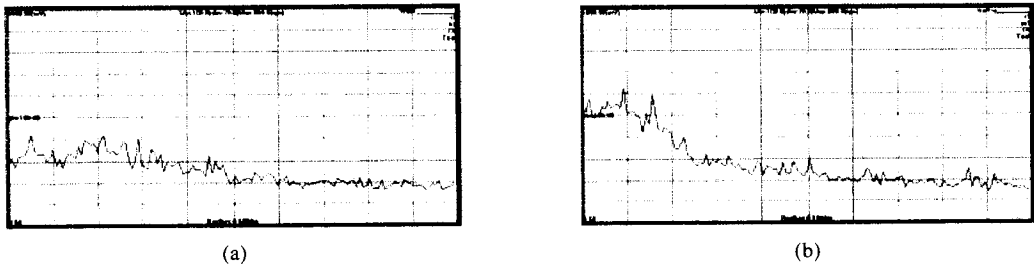

(a)   (b)

Fig. 4 Glide signal for (a) type A disk and (b) type B disk tested with data head
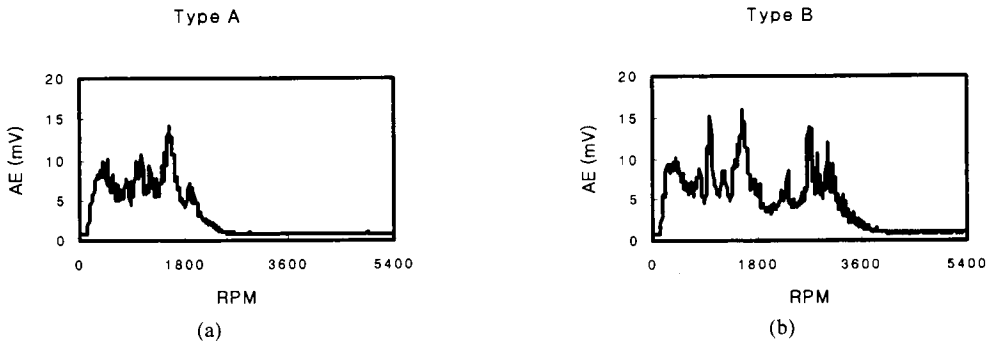

(a)   (b)

Fig. 5 AE signal during take-off of the data head for (a) type A disk and (b) type B disk

susceptible to laser bump excitation. One possible reason for this observation is attributed to the PZT sensor location. For the glide head, the PZT sensor is directly attached to the slider body, on the other hand, for the data head, the PZT sensor, i. e. AE sensor is attached to the suspension of the head assembly. Therefore the glide head is likely to be more sensitive to the laser bump excitation.

Since spectrogram comparison for two different heads could not be made, instead, AE signal was monitored as an alternative method to observe the contact behavior between the laser bump and the head. Figure 5 shows the AE signal for both types of disks tested with the data head. Note that type

B disk produced more high intensity peaks of AE signal up to 3600 rpm, indicating that type B disk generated more contacts during take-off than the type A disk. Therefore it was found that type A disk produced more resonance and contacts for the glide head, on the other hand, type B disk produced more contacts for the data head. This result implies that resonance problem or contact behavior caused by the periodic laser bump depends on the type of the slider body.

Similar results were also observed when pseudo-random laser bump disk was used. It is known that randomization or modulation of the bump array pattern, especially in the circumferential direction, is one effective way to alleviate glide resonance phenomenon. This helps to spread out the periodic input excitation frequencies to avoid system resonance. Figure 6 shows the modulated laser bump pattern in the circumferential direction for type C disk. It has the nominal circumferential pitch of 30 μm, and the circumferential bump pitch changes from 20 μm to 40 μm in a fixed size bin while the pitch between each bin is kept constant. The radial bump pitch is fixed to 20 μm. This bump pattern is called the pseudo-random bump pattern. For comparison with the pseudo-random pattern disk, type D disk of the regular bump pattern was used. It has the same bump density with the pseudo-random disk such as circumferential pitch of 30 μm and radial pitch of 20 μm. Figure 7 shows the spectrogram of pseudo-random bump and regular bump disk respectively when the glide head was used. It is noticed that for pseudo-random bump disk, the

resonance excitation was completely disappeared. Figure 8 shows AE signal of both disks when the data head was used. The intensity of AE signal was not much different from each other, indicating that the severity of contact in the head-disk interface was almost identical for both disks. Again, this implies that higher glide resonance or glide failure is not necessary to lead to head/media interface problem such as wear of laser bump when the data head is used. Resonance problem caused by periodic laser bump pitch
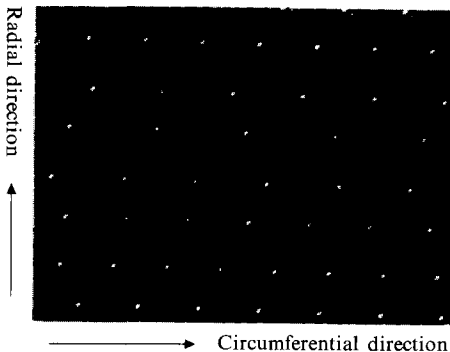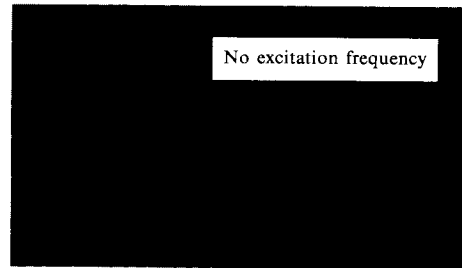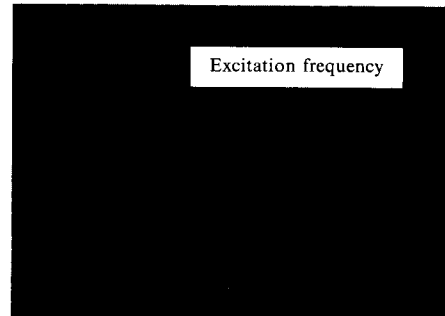

(a)

(b)

Fig. 7 Spectrogram for (a) type C pseudo-random texture disk (b) type D regular texture disk

Circumferential direction

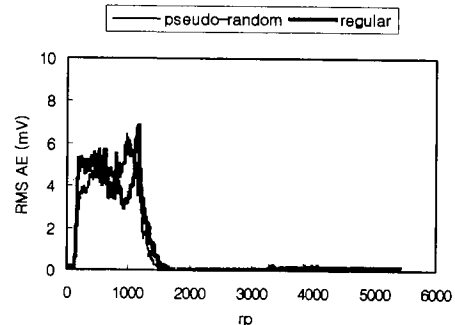**Fig. 6** Pseudo-random bump pattern of type C disk

Fig. 8 AE signal for pseudo-random bump disk and regular bump disk

depends on the type of the slider body, i. e. the natural frequency of the slider used.

On the otherhand, it was not clearly understood why type A disk produced more glide resonance
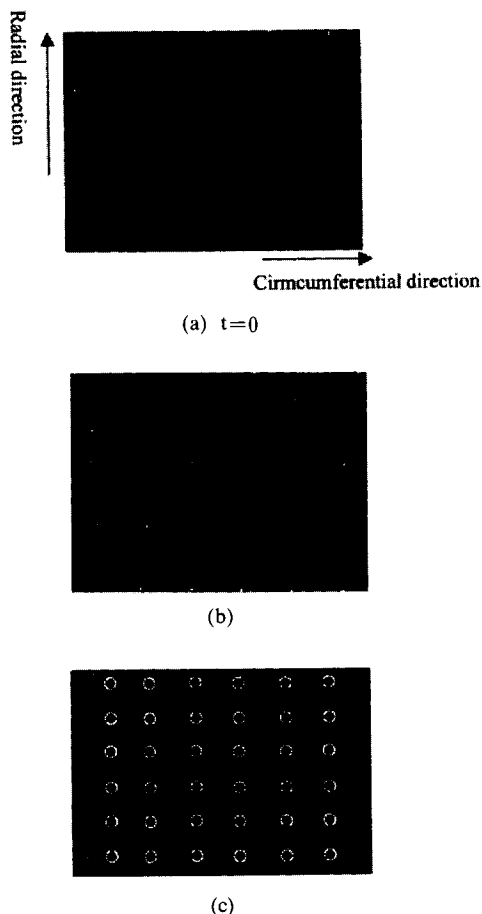

(a) t=0

(b)

(c)

Fig. 9 Laser bump array pattern for (a) type A disk (b) type B disk (c) ideal regular bump pattern disk

than the type B disk. However, we may find the clue in the type of the laser bump array pattern. Figure 9 shows the laser bump patterns for type A, type B, and an ideal rectangular laser bump disks. In an ideal case, the laser bumps will be arranged with square or rectangular pattern. However, for the typical LZT disks, the laser bumps are formed in a spiral pattern and they are not arranged in a rectangular pattern. In this case, bump array will have more than one excited frequency, which will increase the chance of glide resonance. It is because the excited frequencies are related to the number of bumps in the radial direction that passes through the slider every second (Chen et al., 1997). Thus it is thought that type B disk, which has relatively better arranged laser bump pattern in the radial direction than type A disk, produces lower glide resonance.

To further understand the effects of the laser bump pattern on glide avalanche and glide resonance, several samples of the different bump height and pitch were tested. Table 2 shows the bump height and pitch values of the disks tested. For different bump height samples, the results of glide avalanche and AE emission signal during take-off are shown in Table 2 and Fig. 10, respectively. It was observed that as the bump height is decreased, the glide avalanche is greatly reduced and the AE signal intensity is also substantially reduced. This indicates that lower bump height is a key factor in reducing head/media contacts, consequently reducing glide avalanche.

Another way to reduce glide resonance is to make smaller circumferential bump pitch as sug-

Table 2 Design parameters of different bump height and different bump pitch disks tested.

Group A: Different bump height disks			Group B: Different circumferential bump pitch disks		
Bump Spacing: Circ. X Radial (μm)	Bump Height (Å)	Glide Avalanche (μinch)	Bump Spacing: Circ. X Radial (μm)	Bump Height (Å)	Glide Avalanche (μinch)
30×35	150	0.84	10×35	180	1.14
30×35	180	1	20×35	180	0.99
30×35	210	1.2	50×35	180	0.95
30×35	240	1.4			

Different bump height samples

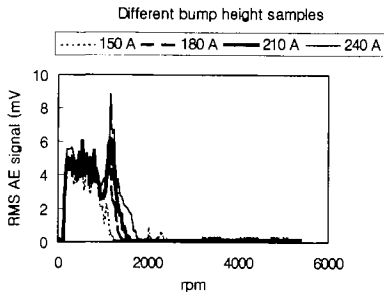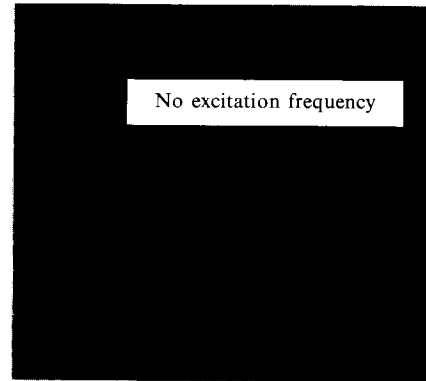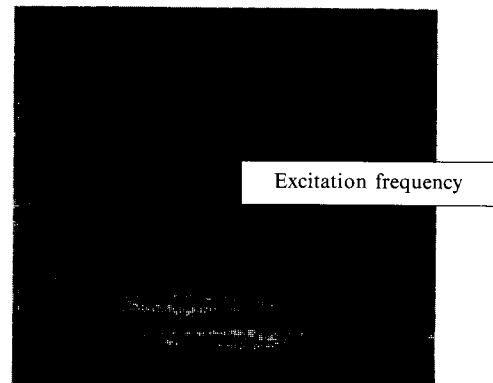······ 150 A — — 180 A ——— 210 A ——— 240 A

Fig. 10   AE signal during take-off for different bump height samples

gested by Yao (1988). The different bump pitch disks listed in Table 2 were tested, and the results of the spectrogram for each disk are shown in Fig. 11. As the bump pitch became smaller, the glide resonance was substantially reduced. However, glide avalanche measurements in Table 2 show that smaller bump spacing produced slightly higher glide avalanche. This was a very interesting observation since we expected that more glide resonance would generate more chance of higher glide avalanche or glide height. However, as bump spacing becomes smaller, the air pressure between neighboring bumps will be increased due to the reduction of effective flow area around the bumps and restrictions in the side–flows (Hu and Bogy, 1997a; 1997b), consequently, leading to increase in the flying height. Therefore, as bump spacing becomes smaller, glide avalanche will be increased due to the air bearing pressure effect even though the chance of high glide resonance will be increased. In summary, lower bump height and larger bump pitch will reduce glide avalanche of the disk. However, bump height plays a more important role in reducing the glide avalanche.
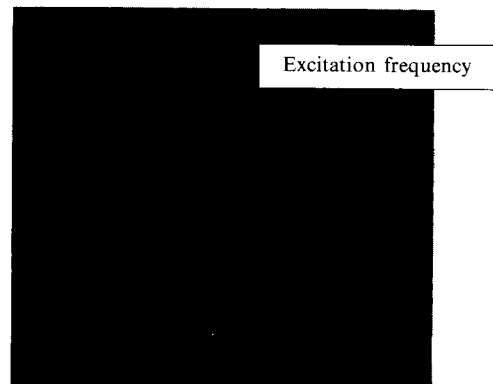
Lowering flying height or glide avalanche generally generates tribological problems such as severe stiction and wear between the slider and the disk. Therefore, a proper laser texture design to balance the lower flying height requirement and tribological concern is always required. Another concern for the laser texture design is the problem of resonance. Even though we found that glide resonance phenomenon during the glide test did not lead to head/media interface problem, the resonance problem of the data head, which has

No excitation frequency

(a) 10 μm disk

Excitation frequency

(b) 20 μm disk

Excitation frequency

(c) 50 μm disk

Fig. 11   Spectrogram of different circumferential bump pitch samples

different resonance frequencies from those of the glide head, still exists. Subsequently the resonance of the data head may generate tribological problem between the head and the disk in real drive operating conditions. Therefore, the laser bump pattern also has to be designed to avoid resonance

of the data head. As described above, it is quite difficult to obtain spectrogram using the data head. However, it is thought that resonance study can be possible through careful investigation of the AE signal as discussed in reference (Knigge and Talke, 1999). Those studies will be performed in the future.

5. Conclusions

(1) The resonance problem caused by the periodic laser bump depends on the type of the slider, that is, the natural frequency of the slider body. Higher glide resonance or glide failure does not necessarily lead to head/media interface problem such as wear of the laser bump in real drive operating conditions where the data head is used.

(2) Laser bump array pattern is also important to reduce glide resonance phenomenon. Ideally rectangular or square bump array pattern is desirable.

(3) Modulated or pseudo-random bump pattern reduces glide resonance effectively. Smaller bump pitch will also help to reduce glide resonance. However, as bump spacing becomes smaller, glide height will be increased due to increased air pressure developed around the bumps. Lowering bump height is the most effective way to reduce glide avalanche.

References

Chen, H., Yu, T., Su, M., Chen, Yi, Yong, P. and Lee, J. K., 1997, "Glide Characteristics of a Laser Textured Disk," *IEEE Trans. Magnetics*, Vol. 33, No. 5., pp. 3103~3105.

Clark, B. K., 1991, "An Experimental Correlation of Slider-Disk Contact Detection between Piezoelectric and Electrical Resistance Measurements," *IEEE Trans. Magnetics*, Vol. 27, No. 6, pp. 5151~5153.

Hu, Y. and Bogy, D., 1997, "Effects of Laser Textured Disk Surfaces on a Slider's Flying Characteristics," *ASME J. of Tribology*, 97-TRIB-18.

Hu, Y. and Bogy, D., 1997, "Flying Characteristics of a Slider over Textured Surface Disks," *IEEE Trans. Magnetics*, Vol. 33, No. 5, pp. 3196~3198.

Knigge, B. and Talke, F. E., 1999, "Acoustic Emission and Stiction Analysis of Patterned Laser Textured Media," *IEEE Trans. Magnetics*, Vol. 35, No. 2, pp. 921~926.

Kuo, D, Gui, J., Marchon, B., Lee, S., Boszormenyi, I., Liu, J. J., Rauch, G. C. and Vierk, S., 1996, "Design of Laser Zone Texture for Low Glide Media," *IEEE Trans. Magnetics*, Vol. 32, No. 5, pp. 3753~3758.

Marchon, B., Kuo, D., Lee, S., Gui, J. and Rauch, G. C., 1996, "Glide Avalanche Prediction From Surface Topography," *ASME J. Tribology*, Vol. 118, pp. 644~650.

Yao, W. H., Kuo, D., Ku, R. and Marchon, B., 1998, "Head-Disc Dynamics of Low Resonances Laser Textures-A Spectrogram Analysis," *IEEE Trans. Magnetics*, Vol. 34, No. 4, pp. 1699~1701.